9.6 SPEED FACTORS AND DEFLECTION ANGLES OF WIND-DRIVEN FLOWS AT THE SEA SURFACE

Yutaka Yoshikawa* and A. Masuda
RIAM, Kyushu University, Kasuga, Fukuoka, Japan

1. INTRODUCTION

The speed factor and deflection angle (referred to as drift parameters for simplicity) of the wind-driven flow has been investigated for long time. It has often been said that the typical speed factor is 0.02–0.03 and the typical deflection angle is 20–30 deg. However, previous observations showed that the speed factor is more likely to range from 0.02 to 0.05 (e.g., Pond and Pickard (1983)) and the deflection angle is less than 45 deg (e.g., Cushuman-Roisin (1994)). In other words, the drift parameters are considerably uncertain.

The main reason for this large uncertainty will be difficulties of the accurate measurements of the wind-driven flow. Wind waves induce instrument motion and wave orbital motion, both of which contaminate the wind-driven flow measurements. Interior currents such as tidal and geostrophic currents are generally larger than the wind-driven flow, and they have to be extracted from the measured velocity to estimate the wind-driven flow. Paucity of the accurate measurements of the wind-driven flow prevents our quantitative understanding of the drift parameters.

Recently developed high frequency (HF) radar is capable of measuring surface velocities without significant wave contamination. The short interval of the measurement ($\sim$ 1 hour) enables accurate estimations of tidal current from tidal harmonic analysis. Given that geostrophic currents were estimated from, for example, sea level differences, ageostrophic current near the surface, a major component of which is the wind-driven flow, can be estimated with good accuracy. The drift parameters can be quantified by comparing the flow with surface winds.

The present study therefore estimates the drift parameters using long (more than 3.5 years) records of velocities measured with HF radar, sea level differences, and analyzed winds. In this paper, two definitions of the drift parameters are used, one uses wind speed and the other uses the (water-side) friction velocity. (The speed factor defined using wind speed (friction velocity) is the ratio of the flow velocity to the wind speed (the friction velocity)). The drift parameters defined using wind speed are useful for comparison with the previous estimations, while the parameters defined using friction velocity are dynamically relevant because the friction velocity is the velocity scale of the wind-driven flow. In this study, particular attention is given to the seasonal variation of the drift parameters and their dependence on the friction velocity.

2. DATA

Data used in the present study are obtained in the eastern channel of the Tsushima Strait (Fig. 1). Five HF radar operate in the channel and there are two sea level stations (Hakata and Izuhara) located across the channel. The accuracy and specifications of these HF radars are described in Yoshikawa et al. (2006). Rectangular ($x-y$) coordinates are assigned in which the x axis is normal to the baseline between the two sea level stations (pointing to the northeast). The period of the data used in this study is from August 1, 2003 to March 31, 2007.

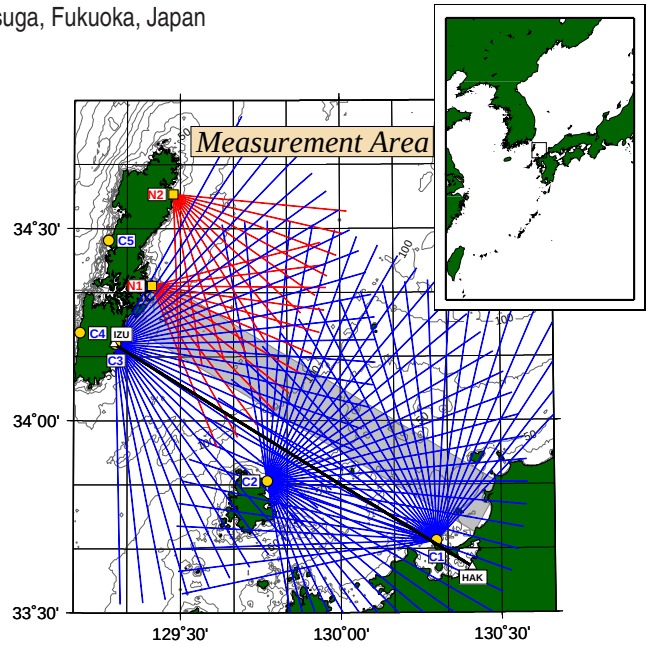

FIG. 1. Locations of HF radar sites (C1∼C3 and N1,N2) and sea level stations (HAK and IZU). Looking lines of the HF radar and the baseline between the two tidal stations are shown by lines. The gray shaded region represents the area in which the surface velocities normal to the baseline are spatially averaged.

a. SURFACE VELOCITY

Tidal components are eliminated from the hourly radial velocities of HF radar using tidal harmonic analysis. From the detided hourly radial velocities, velocities in the x direction (along-channel direction) are calculated at grid points with 0.05° longitude and 0.05° latitude spacing. The velocities are then spatially averaged in the narrow region along the y axis that is indicated by the gray shaded region in Figure 1 to obtain the averaged, detided, hourly surface velocity in the x direction (u_s).

b. SURFACE GEOSTROPHIC VELOCITY

Detided hourly sea level data at Hakata (η_1) and Izuhara (η_2) are used to estimate surface geostrophic velocities (u_g) in the x direction defined as

$$u_g = \frac{g}{fL}(\eta_1 - \eta_2 + \Delta\eta) = u'_g + \frac{g}{fL}\Delta\eta,$$

where g(9.80 m s^{-2}) is the gravity acceleration, f(8.13$\times$10^{-5} s^{-1}) is the Coriolis parameter, L(120 km)

Corresponding author address:Yutaka Yoshikawa, Research Institute for Applied Mechanics, Kyushu Univ., Kasuga, Fukuoka, Japan; e-mail: yosikawa@riam.kyushu-u.ac.jp

is the distance between the two sea level stations, and $\Delta\eta$ is the difference in the base heights of the two stations. ($\Delta\eta$ is unknown and must be estimated in the following analysis.)

c. WIND AND FRICTION VELOCITY

Analyzed surface winds of GPV-MSM published by Japan Meteorological Agency are used in this study. Wind velocities are interpolated to the HF radar grid points (0.05 $\times$ 0.05 deg). The friction velocity is calculated from wind velocities using the drag coefficient formula of Yelland and Taylor (1996). Vector-averages of the wind velocities and the friction velocities are calculated in the narrow region (gray shaded region in Fig. 1) to estimate spatial averages of the wind vector (w_x, w_y) and the friction velocity vector (u_*, v_*).

d. QUALITY CONTROL

To reduce the measurement error and inertially oscillating component (with a period of 21 hours) in the surface velocity (u_s), running means with periods longer than 3 days are applied to all the data. We discard the wind (the friction velocity) if its speed is less than 1.5 m s^{-1} (1.5$\times10^{-3}$ m s^{-1}), because such a small wind speed (or friction velocity) is expected to be less certain.

3. METHODOLOGY

In the present analysis, data are divided into several groups (labeled by m) in which the speed factor α^m and deflection angle θ^m are assumed constant. The wind-driven flow u^n_{wdf} and ageostrophic velocity u^n_{agf} can be expressed as

$$\begin{aligned} u^n_{wdf} &= \alpha^m \cos\theta^m w^{n-h}_x + \alpha^m \sin\theta^m w^{n-h}_y \\ &= a^m w^{n-h}_x + b^m w^{n-h}_y, \\ u^n_{agf} &= u^n_s - u^n_g = u^n_s - u'^n_g + \frac{g}{fL}\Delta\eta = u'^n_{agf} + c, \end{aligned}$$

where h is time lag between wind and the wind-driven flow. (Note that in the above equation, (w_x, w_y) should be replaced with (u_*, v_*) when the drift parameters defined using the friction velocity is estimated.) We assume that a major component of the ageostrophic velocity u^n_{agf} is the wind-driven velocity u^n_{wdf}. Thus a^m, b^m (instead of α^m and θ^m for convenience) and c can be determined such that the square difference between two velocities is minimized.

The validity of the estimation can be examined using the squared correlation between u_{agf} and u_{wdf} (referred to as COR^2) and root mean square of $u_{agf} - u_{wdf}$ (referred to as RMSD). The assumption that a major component of u_{agf} is u_{wdf} means that COR^2, the ratio of the explained variance to the total variance, should be high. In addition, the drift parameters estimated with the running mean periods of 3, 5, 7 and 10 days are compared to examine certainty of the estimation, because the drift parameters estimated with running mean periods much longer than the inertial period should be similar to each other. Time lag is set as 1 hour in this paper because it provides the best correspondence between u^n_{wdf} and u^n_{agf}.

4. RESULTS

a. SEASONAL VARIATIONS

First, data are divided into 12 groups according to their calendar month, and monthly mean of the speed factor (α^m) and deflection angle (θ^m) are investigated. Figure 2 shows the speed factor and deflection angle. Both the speed factor and deflection angle are found to vary seasonally to a considerable degree. The speed factor is 1.13 - 1.34 % in November–February and 1.48 - 2.01 % in June–August. The deflection angle is 14.5 - 27.0 deg in November–February and increases to 40.6 - 65.1 deg in June–August. COR^2 is larger than 0.6 RMSD is smaller than 0.03 m s^{-1} in every months (not shown). Ranges of the drift parameters estimated with different running mean periods are small except in May and September. These indicate that the estimations are reasonable and certain except in May and September.

Note also that similar seasonal variations are found in the drift parameters defined using the friction velocity (not shown). The speed factor is 8.9–10.2 in November–February and 11.3–15.3 in June–August. The deflection angle is 15.8–26.0 deg in November–February and increases to 39.6–64.7 deg in June–August.

b. DEPENDENCE ON FRICTION VELOCITY

The dependence of the drift parameters on the friction velocity was examined by dividing data into 10 groups based on the magnitude of the friction velocity with 1 $\times10^{-3}$ m s^{-1} intervals. Taking account of their large seasonal variation, the drift parameters in summer (June–August) and winter (November–February) are separately analyzed. Figure 3 shows the estimated drift parameters in summer and winter. Noteworthy is that clear dependence of the drift parameters on the friction velocity is found in winter; The speed factors in the data groups with COR^2 $\geq$ 0.5 (in which the estimation is reasonable) increase with the friction velocity, while the deflection angles in these groups decrease slightly or change little with the friction velocity. Small ($\leq$ 1.7$\times10^{-2}$ m s^{-1}) RMSD and small ranges of parameters estimated with different running mean periods suggest that the dependence is considerably certain.

We also investigated the dependence of the drift parameters on the wind direction by dividing data into eight groups based on the wind direction. However, no significant dependence was found.

5. DISCUSSION

The profile of wind-driven flow (and hence the drift parameters) depends on the eddy viscosity profile. The eddy viscosity profile varies seasonally due to seasonal variation of stratification and heat flux. To examine whether seasonal variation of eddy viscosity can induce the seasonal variation of the drift parameter estimated in the previous section, the wind-driven flow profiles was simulated by solving

$$f(-v(z), u(z)) = \frac{d}{dz}\left(\nu(z)\frac{d}{dz}(u(z), v(z))\right),$$

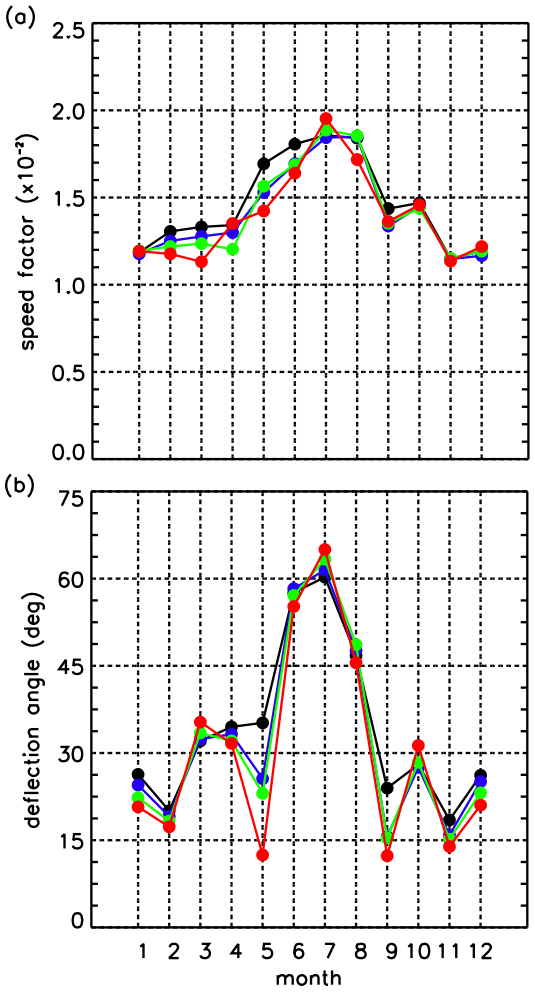

FIG. 2. (a) Speed factor (α^m) and (b) deflection angle (θ^m) estimated from monthly analysis. Color indicates running mean periods (black: 3 days, blue: 5 days, green: 7 day and red: 10 days). Estimations with $\mathrm{COR}^2 \geq 0.5$ are marked by solid circle.

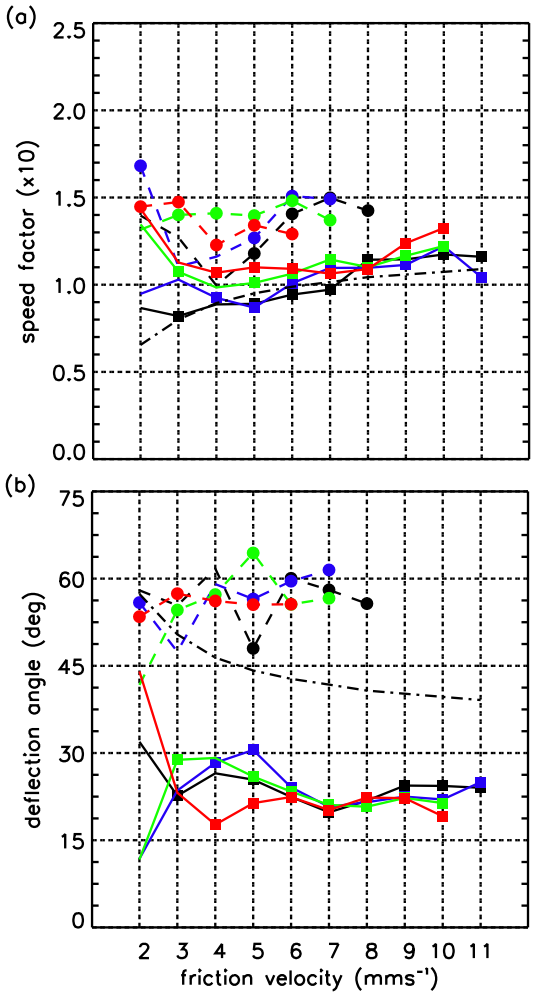

FIG. 3. Same as Fig. 2 but as a function of the friction velocity. Dashed and solid lines show estimations in summer (June–August) and winter (November–February), respectively. Dash dotted lines show the speed factor and deflection angle calculated from the simulated wind-driven flow in winter (see section 5).

with boundary conditions

$$\begin{aligned} \nu(z)\tfrac{\partial}{\partial z}(u,v) &= (0,U_*^2) \quad \text{at } z=0, \\ (u,v) &= (0,0) \quad \text{at } z=-U_*/f, \end{aligned}$$

and with eddy viscosity profiles for summer and winter. The depth of the model ocean (U_*/f) is 123 m for $U_* = 0.01$ m s^{-1} in the Tsushima Strait (f=8.13$\times$10^{-5} s^{-1}), where the typical water depth is about 100 m. The above equation is solved using a second-order finite difference scheme with 500 uniform grids. The drift parameters defined using the friction velocity are then calculated from the simulated wind-driven flow.

As the eddy viscosity profile for winter, the piece-wise linear profile proposed by Zikanov et al. (2003) (referred to as profile Z, Fig. 4a) is used, who performed a large-eddy simulation (LES) of a turbulent wind-driven flow in a homogeneous fluid. As the eddy viscosity profile for summer, the piece-wise linear profile similar to the profile inferred by Yoshikawa et al. (2007) from the measured velocity spiral in the summer Tsushima Strait is used (referred to as profile Y). We also use a slightly different profile of the eddy viscosity (profile X) in which the subsurface eddy viscosity is smaller than that in profile Y (Fig. 4a), which is meant to represent the eddy viscosity in a more stratified situation.

The speed factor and deflection angle (defined using the friction velocity) for the velocities simulated using profiles X and Y (corresponding to the summer profile) at the surface are 11.9 and 58.3 deg and 15.0 and 61.6 deg, respectively, while the speed factor and deflection angle for the velocity simulated using profile Z (corresponding to the winter profile) are 12.2 and 34.8 deg at the surface (Fig. 4b). The differences in the simulated drift parameters for summer and winter are as large as the difference estimated in the previous section. Thus, the present estimation indicates that the seasonal change in the eddy viscosity is a likely cause of large seasonal variations of the drift parameters.

The simulated wind-driven flow profile can be used to examine the dependence of the drift parameters on the friction velocity. The depth of the wind-driven flow (U_*/f) changes with friction velocity, while the depth of an HF radar measurement ($\leq$ 2 m)

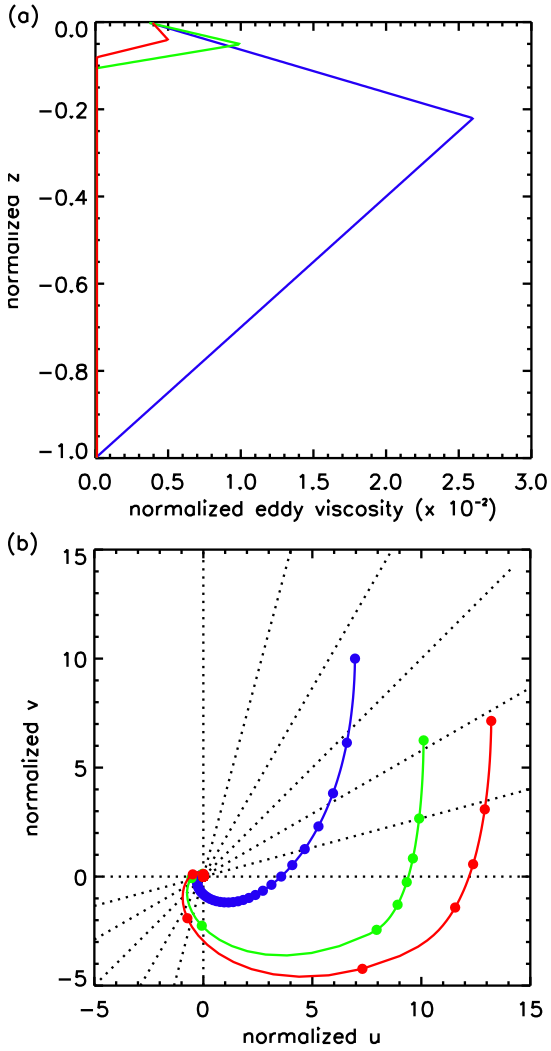

FIG. 4. (a) Profiles of the eddy viscosity and (b) hodographs of the simulated wind-driven flows. Blue, green, red lines represent the profile Z, Y, and X, respectively. Solid circles are plotted with 0.02 (normalized) depth intervals.

is unchanged. Thus the HF radar tends to measure a shallower part of the wind-driven flow as the friction velocity increases. To examine this effect, the drift parameters at the HF radar measurement depth are calculated from the velocity profile simulated with the several friction velocity. Results are shown by dash dotted lines in Figure 3. The simulated speed factor explains well with the estimated. The simulated deflection angle is larger than the estimated by 17 deg. However, this difference is due largely to the approximated representation of the piece-wise linear profile of the eddy viscosity (Zikanov et al. (2003)). This indicates that the dependence of the wind-driven flow depth on the friction velocity likely causes the dependence of the drift parameters on the friction velocity.

6. CONCLUDING REMARKS

Large seasonal variations in both the speed factor and deflection angle (drift parameters) and clear dependence of the drift parameters on the friction velocity are found. The seasonal variation of the eddy viscosity profile is likely cause of the seasonal variation of the drift parameters, while the change in the wind-driven flow depth (U_*/f) with the friction velocity is possible cause of the dependence on the friction velocity. Although these effects qualitatively explain the estimated variations of the drift parameters, we do not state that other effects such as surface waves do not play roles in determining the wind-driven flow profile and drift parameters. To clarify these processes with field experiments, more detailed and precise measurements of wind-driven velocities for several depths, wind stresses, and heat fluxes are needed.

We finally remark that the speed factor is usually less than the typical speed factor (0.02–0.03) and that the deflection angle is much larger than the typical angle (20–30 deg) in summer. Such large differences result in large differences of the drift velocities (e.g., 7 km per day or 110 miles per month in December). It is also noteworthy that accurate estimation of the wind-driven flow using the drift parameters allows estimations of the interior current field from the surface currents measured with HF radar. This is useful to identify causes of current variations measured with HF radar.

REFERENCES

Cushuman-Roisin, B., 1994: *Introduction to Geophysical Fluid Dynamics*. Prentice-Hall, 320pp pp.

Pond, S. and G. L. Pickard, 1983: *Introductory Dynamical Oceanography*. Butterworth-Heinemann, 329pp pp.

Yelland, M. and P. K. Taylor, 1996: Wind stress measurement from the open ocean. *J. Phys. Oceanogr.*, **26**, 541–558.

Yoshikawa, Y., A. Masuda, K. Marubayashi, M. Ishibashi, and A. Okuno, 2006: On the accuracy of of hf radar measurement in the tsushima strait. *J. Geophys. Res. Oceans*, **111**, C04009, doi:10.1029/2005JC003232.

Yoshikawa, Y., T. Matsuno, K. Marubayashi, and K. Fukudome, 2007: A surface velocity spiral observed with adcp and hf radar in the tsushima strait. *J. Geophys. Res. Oceans*, **112**, C06022, doi:10.1029/2006JC003625.

Zikanov, O., D. Slinn, and M. Dhanak, 2003: Large-eddy simulations of the wind-induced turbulent ekman layer. *J. Fluid Mech.*, **495**, 343–368.